Journal of Photochemistry and Photobiology A: Chemistry 221 (2011) 175–180

Contents lists available at ScienceDirect

Journal of Photochemistry and Photobiology A: Chemistry

journal homepage: www.elsevier.com/locate/jphotochem

Surface-enhanced Raman scattering at well-defined single crystalline faces of platinum-group metals induced by gap-mode plasmon excitation

Katsuyoshi Ikeda [a,b,*], Jun Sato [a], Kohei Uosaki [a,b,c,**]

[a] Division of Chemistry, Graduate School of Science, Hokkaido University, Sapporo 060-0810, Japan
[b] Global Research Center for Environment and Energy based on Nanomaterials Science (GREEN), National Institute for Materials Science (NIMS), Sapporo 060-0810, Japan
[c] International Center for Materials Nanoarchitechtonics (MANA), National Institute for Materials Science (NIMS), Tsukuba 305-0044, Japan

ARTICLE INFO

Article history:
Available online 25 February 2011

Keywords:
Surface enhanced Raman scattering
Self-assembled monolayer
Platinum

ABSTRACT

It is normally difficult to use surface enhanced Raman scattering (SERS) to study molecular adsorbates at well-defined planar metal surfaces or at Pt-group catalytic metal surfaces. In this paper, highly localized gap-mode plasmons are excited on atomically smooth metal surfaces by using a sphere-plane type plasmonic cavity. This method enables us to observe Raman scattering signals from molecular adsorbates on various single crystalline metal surfaces including non-SERS-active Pt and Pd. SERS spectra of self-assembled isocyanide monolayers on several metal substrates with (1 1 1) or (1 0 0) orientation reveal a significant orientation dependence of preferential adsorption sites, which information is hardly obtainable from conventional SERS spectra.

1. Introduction

Surface enhanced Raman scattering (SERS) is widely recognized as a powerful spectroscopic tool for studying molecular adsorbates on a metal surface [1,2]. The surface enhancement of Raman signals is mainly caused by electromagnetic field enhancement near a metal surface via excitation of surface plasmon polaritons. After the discovery of the SERS effect [3–5], significant efforts have been made to increase the efficiency of the enhancement effect, and then, the enhancement factor (EF) of Raman signals is now approaching to the order of 10^{14}, implying a possible application to single molecular detection [6,7]. Due to the enhancement mechanism, however, the practical use of SERS is limited by plasmonic nature of metal substrates. For example, plasmon excitation requires matching the wave vectors of the exciting light and the plasmon modes, and hence, SERS experiments have been usually carried out at electrochemically roughened metal surfaces [1,2]. However, various adsorption sites are exposed on such surfaces, and thus information of each adsorption site is not available from conventional SERS spectra. Moreover, surface enhancement at roughened metal surfaces is only strong on coinage metals such as Au, Ag, and Cu. This limitation severely reduces the range of application of SERS; most of other metals, including catalytic metals such as Pt or Pd, are commonly considered to be non-SERS-active [8–10]. This is because efficient excitation of surface plasmons is difficult on such a highly damping metal surface. Pt-group metals are one of most important catalytic metals and are now indispensable for operation of fuel cells and for purification of automotive exhaust gas. It is therefore essentially important to study how molecules interact with a specific crystal face or a defect-site of these catalysts. In this sense, it would be helpful to develop a convenient method to induce SERS effects at an atomically well-defined surface of non-SERS-active metals.

One of the enhancement techniques for observing a planar surface of single crystalline metals is the attenuated total reflection (ATR) method at Otto configuration [9]. However, the signal enhancement available in this method is not so large because its field localization is limited to only one direction normal to the surface. Tip-enhanced Raman spectroscopy (TERS) also enables us to observe Raman signals at a smooth metal surface [11], but it is still technically difficult to obtain reproducible enhancement especially on an opaque substrate. On the contrary, we have recently reported a convenient technique to form a plasmonic cavity on atomically smooth single crystalline metal substrates and demonstrated significant efficiency enhancement of Raman scattering [12–15] and photochemical reactions [16]. This method is based on excitation of highly localized gap-mode plasmons using a sphere-plane type metal nano-structure, which was theoretically proposed by Aravind and Metiu [17,18]. In addition to the highly repro-

* Corresponding author at: Division of Chemistry, Graduate School of Science, Hokkaido University, Sapporo 060-0810, Japan.
** Corresponding author at: International Center for Materials Nanoarchitechtonics (MANA), National Institute for Materials Science (NIMS), Tsukuba 305-0044, Japan.
E-mail addresses: kikeda@pchem.sci.hokudai.ac.jp (K. Ikeda), UOSAKI.kohei@nims.go.jp (K. Uosaki).

1010-6030/$ – see front matter © 2011 Elsevier B.V. All rights reserved.
doi:10.1016/j.jphotochem.2011.02.022

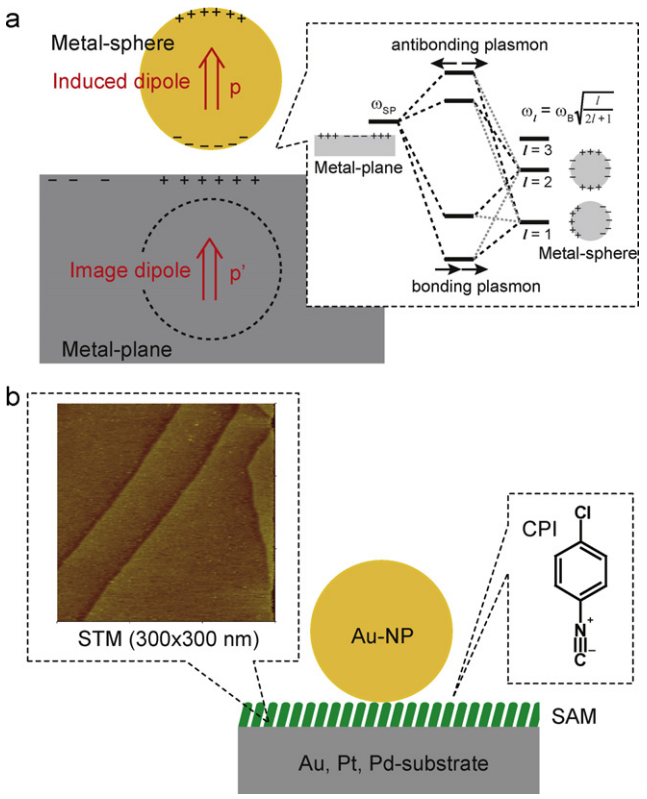

Fig. 1. (a) Schematic illustration of a sphere-plane plasmonic cavity. Inset: energy diagrams for plasmon hybridization between the sphere and the metal. (b) Schematic illustration of an experimental system using the sphere-plane cavity in order to increase Raman signal intensities from organic monolayers at single crystalline metal surfaces. The inset shows a STM image of Pt(1 1 1) surface with monoatomic step-terrace structures.

ducible enhancement [15,19], the other remarkable advantage in this method is that the plasmonic enhancement is available even at a non-SERS-active Pt surface [13]. This is because localized plasmons less decay on a highly damping metal surface than propagating surface plasmons. A similar technique for observation of Pt surfaces was lately reported by Tian et al. [20].

In this paper, we report gap-mode enhanced Raman spectra for self-assembled arylisocyanide monolayers adsorbed on (1 1 1) and (1 0 0) faces of single crystalline metal substrates, SERS-active Au, and non-SERS-active Pt and Pd. We demonstrate that conventional SERS spectra at a rough surface with various adsorption sites can be decomposed to spectral components at the single crystal surfaces with the respective crystal orientation. It is highly advantageous to be able to observe Raman signals of molecules adsorbed on a well-defined surface to study metal–molecular interactions and reaction mechanisms on these catalytic metals.

2. Methodology

2.1. Theoretical background of sphere-plane type plasmonic cavity

Fig. 1a shows a schematic illustration of a sphere-plane type plasmonic cavity, which consists of a metal nano-sphere and a metal planar substrate. In the absence of the sphere, surface plasmons cannot be excited at the planar surface because wave vectors of surface plasmons are not matched with those of photons. However, the presence of the sphere breaks the translational symmetry along the surface, resulting in making plasmon excitation allowed [17,18]. This situation can be understood as follows: the incident light field polarizes the sphere. This polarized field corresponds to dipolar plasmons ($l = 1$). When the sphere is placed close to the surface, it is polarized by its image field, which is realized as localized surface plasmons, in addition to the polarization by the incident field. Since the image field is spatially inhomogeneous, it can excite multipolar plasmons ($l = 2, 3\ldots$) in the sphere. As a result of the electromagnetic interactions between the sphere and the substrate, hybridized bonding plasmon modes are built, which are called gap-mode plasmons. Importantly, gap-mode plasmons are accompanied with highly localized electromagnetic fields in the gap region between the sphere and the plane with the volume of $\sim nm^3$, and hence, huge enhancement of Raman scattering intensity is expected via excitation of the modes.

2.2. Experimental details

The sphere diameter and the sphere-plane distance are important parameters to determine the degree of plasmon hybridization in the cavity. Therefore, it is indispensable to use monodispersed metal nanoparticles (NPs) experimentally. The latter is also precisely controllable if our concern is a well-defined metal-molecular interface such as a self-assembled monolayer (SAM) formed on a single crystalline metal surface. As shown in Fig. 1b, a large number of sphere-plane cavities can be constructed by physisorption of Au-NPs onto the SAM-covered metal substrate with the gap distance determined by the monolayer thickness.

The experimental procedure for sample preparation is as follows [12,13]. Au, Pt, and Pd single crystalline microbeads, having atomically flat (1 1 1) and (1 0 0) facets, were prepared by Clavilier method [21]. Additional annealing for Pt and Pd microbeads was carried out at 1600 °C for 6 h and at 1200 °C for 2 h, respectively, under argon/hydrogen flow by using an induction heater (HOTSHOT-2kW, Ameritherm). These surfaces were then immediately protected by a hydrogen-saturated pure water droplet. Fig. 1b inset is a typical STM image of Pt(1 1 1), showing the well-defined monoatomic step-terrace structure. Next, these beads were immersed in a THF solution containing 10 mM 4-chlorophenylisocyanide (CPI, Oakwood products) to form CPI-SAMs on their surfaces under argon atmosphere. Finally, these SAM-covered metal beads were dipped in a colloidal solution of citrate-reduced Au-NPs with diameter of ca. 20 nm so that the Au-NPs were adsorbed on the organic layers [12,13]. In order to compare the gap-mode enhanced Raman spectra with conventional SERS spectra, electrochemically roughened substrates of Au, Pt, and Pd were also prepared by application of oxidation reduction cycles in KCl solution and H_2SO_4 solution, respectively.

A microscope system was used to observe Raman scattering signals from each facet selectively. The sample was illuminated through an objective lens (40×, 0.6 N.A.) by 632.8-nm radiation with intensity of 0.02 mW from a He–Ne laser, and back-scattered Raman signals were collected with the same objective lens and monitored by a CCD-polychromator system (PIXIS 400B, Princeton Instruments) after Rayleigh scattering light was filtered by an edge filter (Semrock). Note that the tight focusing with the high N.A. object lens is essentially important to excite gap-mode plasmons efficiently.

2.3. Computational details

The plasmon hybridization with Au-sphere and the respective metal substrate was evaluated by theoretical calculations of extinction and field enhancement in the sphere-plane system. The calculation was carried out under a static field approximation according to Wind's method [22,23]. In the calculation, we assumed

an Au-sphere with a diameter of 20 nm above a planar substrate of Au, Pt, or Pd with the separation of 1 nm. By considering the presence of the organic layer on the substrate surface, the refractive index of 1.5 was assumed for the environment. The incident light was *p*-polarized with the angle of 45 degree normal to the surface and the observation point was in the plane of the incidence. The field enhancement was computed at a point located on the symmetry axis of the system at the substrate surface. The convergence of the calculated values was maintained by taking into account 100th-order multipole interactions.

Raman-active vibrational modes of CPI adsorbed on each metal surface were calculated by using Gaussian 09 Revision A02 with the density functional method at the B3PW91 level of theory with LanL2DZ basis set for metal atoms and 6-31G** basis sets for other atoms. A metal cluster such as $(Pt)_3$ was used as a substrate model in the calculation.

3. Results and discussion

3.1. Plasmonic resonance property

Fig. 2a shows optical constants of Au, Pt, and Pd, which were taken from the literatures [24,25]. The negative values of the real part of the permittivity indicate that surface plasmons can be excited on these metals when the wave vectors of photons and plasmons are matched. From the imaginary part of the permittivity, however, one can see that Pt and Pd are highly damping in the entire wavelength region; only the Au surface is thought to be SERS-active below 500 nm when the substrate is roughened. This is indeed confirmed by the calculated extinction spectra of an isolated sphere of these metals with diameter of 20 nm. As shown in Fig. 2b, Pt- and Pd-NPs show no plasmonic feature in the visible region while the Au-NP reveals a plasmon resonance peak around 535 nm.

The degree of the plasmon hybridization in the sphere-plane cavity is largely affected by its substrate metal (only the Au-sphere is considered in this work). More specifically, it is characterized by plasma frequency of the substrate metal. Generally, contributions from the higher-order multipole plasmons to the bonding gap-mode plasmons become stronger with increasing the plasma frequency [26]. According to the Drude model parameter fitting, the plasma frequencies of Au, Pt, and Pd are calculated to be 7.28, 4.15, and $4.40 \times 10^4\,cm^{-1}$, respectively [27]. Therefore, the plasmon hybridization of a Pt or Pd substrate with an Au-NP is thought to be weaker than that of an Au substrate. We calculated extinction spectra of an Au-NP above each metal substrate. In the calculation, the sphere-plane distance was set to 1 nm by considering a typical thickness of organic monolayers [28]. As shown in Fig. 2b, the plasmon resonance of the Au-NP is largely shifted to 640 nm in the presence of the Au-substrate, indicating the strong plasmon coupling between these metals. On the other hand, the resonance peak is found to be around 590 nm when located near the substrate surface of Pt or Pd. Although the smaller red-shift of the plasmon resonance suggests the weaker electromagnetic coupling, one can still expect that Raman scattering intensity is substantially enhanced in the sphere-plane cavity. Fig. 2c shows spectra of EFs in the sphere-plane cavity calculated for the respective substrate metal; in the calculation we assumed that the EF was nearly proportional to the fourth power of the field enhancement, $|E/E_0|$, where E and E_0 denote the enhanced local field and the incident field, respectively [29]. Since the EF value becomes more than 10^6 around 600 nm even on the Pt and Pd substrates in the presence of the Au-NP, the enhanced Raman signals should be detectable when the system is excited by the 632.8 nm radiation from a He–Ne laser.

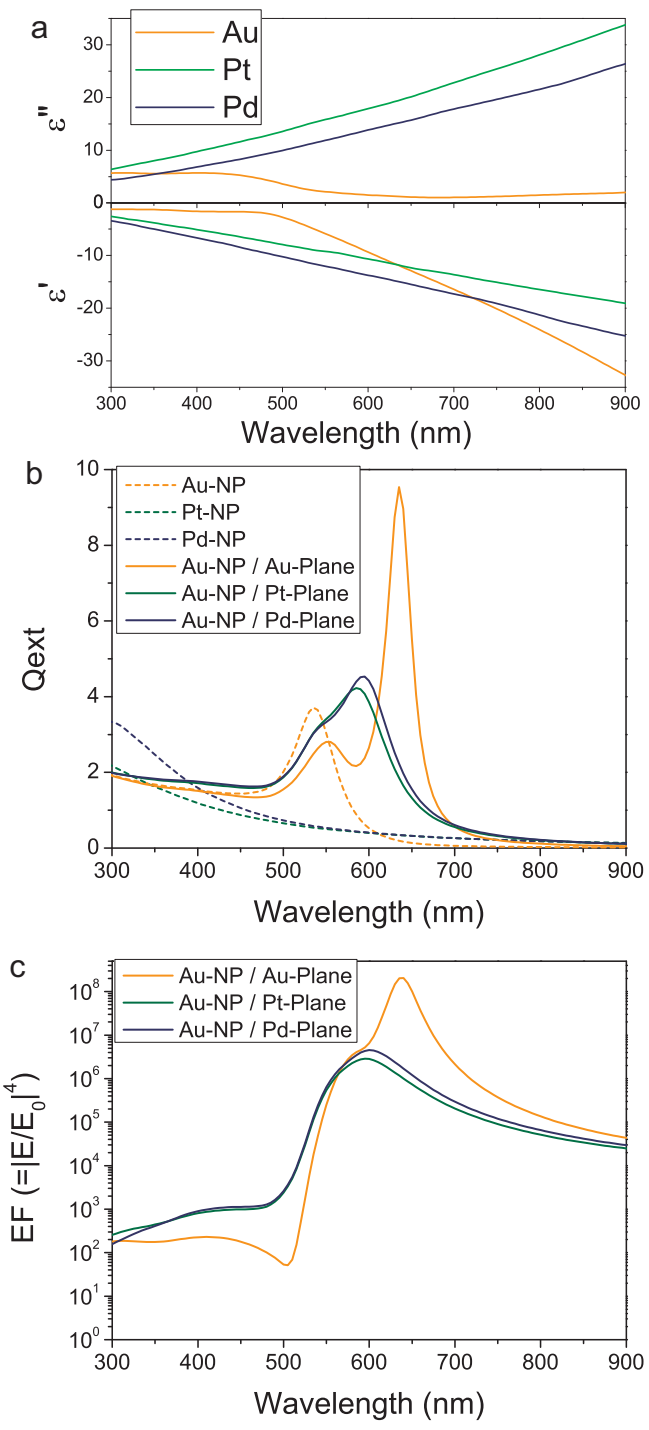

Fig. 2. (a) Wavelength dependence of optical constants for Au, Pt, and Pd [25,26]. (b) Calculated extinction spectra of a nanosphere of Au, Pt, and Pd (Au-NP, Pt-NP, and Pd-NP), and of an Au-NP above a substrate of Au, Pt, and Pd (Au-NP/Au-Plane, Au-NP/Pt-Plane, and Au-NP/Pd-Plane). The diameter of the Au-NP and the sphere-plane distance were assumed to be 20 nm and 1 nm, respectively. The incident angle was 45 degree with respect to the normal to the surface. (c) Enhancement factors as a function of the incident wavelength in the sphere-plane systems calculated at the point located on the symmetry axis of the system at the substrate surface.

3.2. Conventional SERS spectra of self-assembled CPI monolayers on roughened surfaces

Fig. 3 shows typical SERS spectra of CPI-SAMs on electrochemically roughened surfaces of polycrystalline Au, Pt, and Pd. On the roughened Au surface, Raman active modes of CPI were clearly

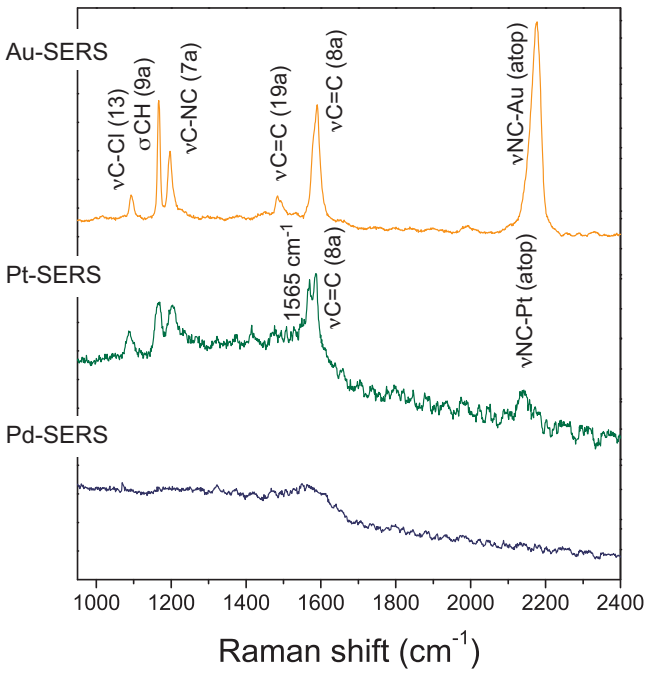

Fig. 3. Conventional SERS spectra of CPI-SAMs on electrochemically roughened Au, Pt, and Pd surfaces.

observed in the spectrum [13,30–33]. The NC stretching frequency (νNC) of 2180 cm^{-1} indicates the bond formation between the isocyano anchor group and the substrate [12]. Although the surface roughening by repetitive potential cycling was less effective for so-called "non-SERS-active" Pt and Pd substrates, we were somehow able to obtain the distinct Raman bands of CPI on the roughened Pt surface. The νNC frequency of 2144 cm^{-1} on Pt was slightly lower than that on Au, indicating the substrate dependence of the NC chemisorption strength, which will be discussed later. Moreover, a significant difference was found around νC=C frequency region. In addition to the totally symmetric νC=C (8a) mode at 1586 cm^{-1}, an additional peak appeared at 1565 cm^{-1}, which was close to the position of the non-totally symmetric νC=C (8b) mode [13]. Actually, spectral reproducibility was significantly low at Pt; especially these two peaks varied its relative intensities to a large extent. Note that roughened surfaces by electrochemical potential cycling have a wide distribution of surface features with various adsorption sites exposed. It is naturally expected that such uncontrolled surface features result in low reproducibility in SERS spectra. As for Pd, we could not obtain any distinguishable Raman band by the surface roughening.

3.3. *Crystal orientation dependence of CPI adsorption geometry on various metal surfaces*

The use of the sphere-plane type plasmonic cavity enables us to observe Raman spectra from a well-defined single crystalline metal surface. As expected from the theoretical calculations in Fig. 2, similar signal intensity was obtained from Pt and Pd surfaces. According to the previous estimation of the EF on Pt [13], the EF on Pd is also estimated to be the order of 10^5. Fig. 4a shows gap-mode enhanced Raman spectra of CPI-SAMs at (1 0 0) faces of each metal substrate. All of the Raman bands appeared in these spectra was ascribed to the vibrational modes of the CPI. The assignment of the bands is summarized in Table 1, together with our DFT calculation results. Among these Raman active bands, the most characteristic vibration is the stretching mode of the NC group because the frequency of this mode is highly sensitive to substrates as already shown in the conventional SERS spectra. In the case of the Au(1 0 0), the νNC-Au vibration was found to be around 2185 cm^{-1}, which corresponds to the atop configuration [30–33]. On the other hand, the spectrum at Pd(1 0 0) showed the vibration peak with the lower frequency of 1969 cm^{-1}, indicating the presence of the bridge-bound CPI [32,33]. Note that there is no νNC-Au peak found at the Pd(1 0 0), suggesting the chemically bound inter-

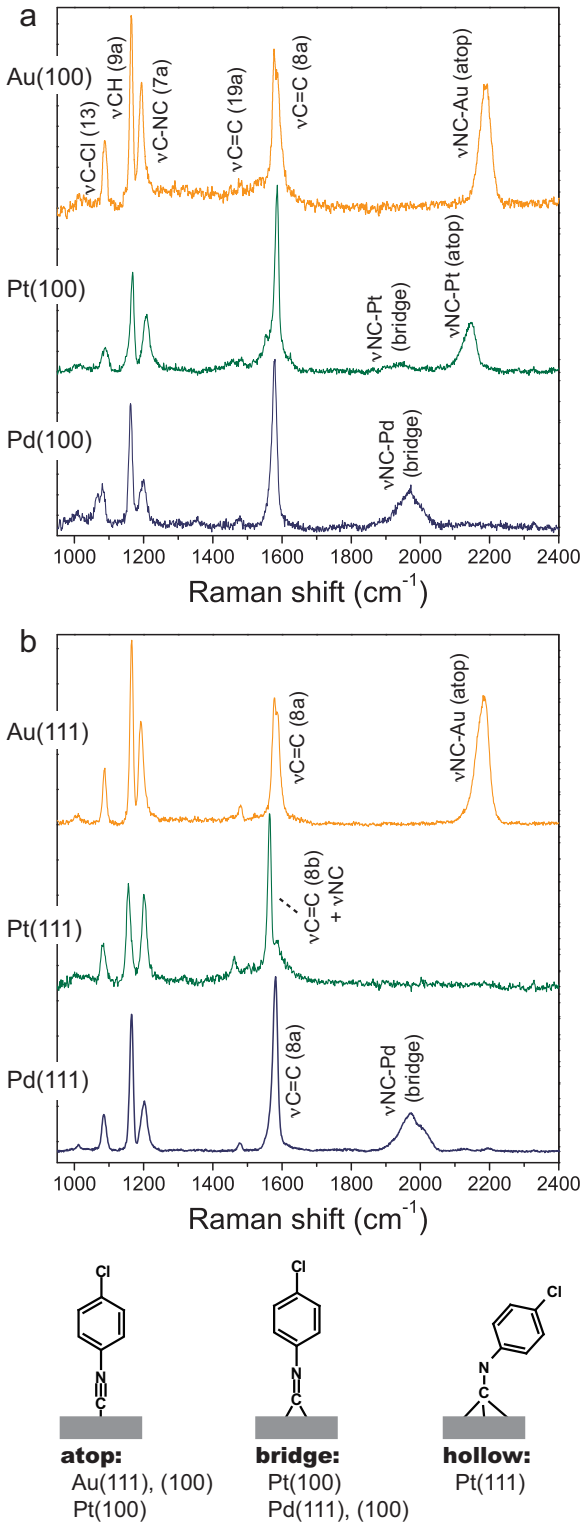

Fig. 4. Gap-mode plasmon enhanced Raman spectra of CPI-SAMs on (a) Au(1 0 0), Pt(1 0 0), and Pd(1 0 0) and on (b) Au(1 1 1), Pt(1 1 1), and Pd(1 1 1).

Table 1
Vibrational frequencies (cm^{-1}) of CPI adsorbed on Au, Pt, and Pd substrates.

	Au			Pt					Pd		
	(1 0 0) exp.	(1 1 1) exp.	Atop calc.	(1 0 0) exp.	(1 1 1) exp.	Atop calc.	Bridge calc.	Hollow calc.	(1 0 0) exp.	(1 1 1) exp.	Bridge calc.
νC-Cl(13)	1087	1088	1080	1089	1084	1079	1075	1073	1080	1085	1085
σCH(9a)	1165	1165	1150	1168	1156	1151	1147	1142	1162	1165	1147
νC-NC(7a)	1192	1191	1205	1208	1201	1226	1222	1202	1198	1201	1215
νC═C(19a)	1478	1480	1470	1482	1461	1471	1464	1460	1479	1479	1466
νC═C(8b) + νNC			–	–	1564	–	–	1574			
νC═C(8a)	1577	1578	1593	1586	1585	1596	1588	1622	1580	1581	1591
νNC-M	2185	2185	2194	1939, 2145	–	2146	1932	–	1969	1972	1981

face of the CPI-SAM/Pd substrate is maintained after the adsorption of Au-NPs onto the CPI monolayer. Conversely, the Pt(1 0 0) exhibited both of the atop and bridge features in the νNC vibration region. According to the relative intensity between these two modes, one can conclude that the CPI molecules prefer atop sites but can also adsorb at bridge sites on this surface. The slight difference in the atop vibration frequencies between Au and Pt, about 40 cm^{-1}, can be explained by the difference in the degree of π back-donation; the LUMO of CPI is a π^*-orbital that is anti-bonding with respect to the NC bond and any electron donation into this orbital from metal d_π-orbitals leads to a decrease in the νNC frequency [31–33]. That is, the back-donation is stronger at Pt(1 0 0) than at Au(1 0 0). The difference in the bridge vibration frequencies between Pt and Pd can be also explained in a similar manner, the stronger back-donation at Pd(1 0 0) than at Pt(1 0 0). Interestingly, the Pt(1 0 0) spectrum did not show 1565 cm^{-1} peak found in the conventional SERS.

Gap-mode enhanced Raman spectra of CPI-SAMs were also measured at (1 1 1) faces of each metal substrate as shown in Fig. 4b. As for the Au and Pd, no crystal orientation dependence was observed in the spectra; the preferential adsorption site was the atop at Au, and the bridge at Pd. On the contrary, Pt showed significant crystal orientation dependence. The spectral appearance at Pt(1 1 1) was actually largely different not only from that at Pt(1 0 0) but also from all others, which was characterized by the absence of the νNC vibration and by red-shift of the νC═C vibration. In the previous paper [13], these features were tentatively ascribed to N-protonation of CPI molecules [34–36]; the bent configuration between the aromatic-ring and the isocyano group induces coupling of νNC vibration and the νC═C vibration, resulting in the intensity lost of the νNC vibrations and the totally symmetric νC═C (8a) and, and the intensity gain of the non-totally symmetric νC═C vibration (8b). As a result of further detailed DFT calculations, however, we found that a similar bent configuration can be stable at hollow sites of the Pt(1 1 1). Although we cannot experimentally determine which is the true adsorption structure at the present stage, the hollow-bound CPI is naturally assumed to be the preferential adsorption at Pt(1 1 1).

Here, it should be noted that the spectral feature of the conventional SERS on the roughened Pt can be reproduced as a sum of the gap-mode enhanced Raman spectra on Pt(1 1 1) and Pt(1 0 0). The low reproducibility of the Pt-SERS spectra can be then explained by the difference in the ratio of (1 1 1)- and (1 0 0)-features on the roughened surface. On the other hand, the relatively reproducible spectral feature of the conventional SERS on the roughened Au can be explained by the fact that the adsorption geometry did not show any remarkable crystal orientation dependence between (1 1 1) and (1 0 0). One can conclude that the gap-mode plasmon excitation method can indeed provide well-resolved information of metal-molecule interactions at a specific surface site whereas conventional SERS spectra give us only averaged information of various surface features. This must be a significant advantage to study adsorption behavior or reaction mechanism of molecules at a catalytic metal surface.

Next, we focus to compare the adsorption geometries of the CN group with those of CO. In the field of catalytic chemistry, the CO adsorption on Pt-group metals has been extensively studied by infrared reflection absorption spectroscopy (IRAS) and by theoretical methods [37–40]. It has been reported that CO preferentially adsorbs at the atop sites of Au(1 1 1) and (1 0 0) and the bridge sites of Pd(1 1 1) and (1 0 0). Coexistence of the atop and bridge CO on Pt(1 0 0) is also confirmed experimentally. Therefore, the adsorption behavior of the CN group seems to be very similar to that of CO. Conversely, the situation on Pt(1 1 1) is rather complicated. Actually, the CO adsorption on Pt(1 1 1) is still in a puzzled situation; CO is experimentally found at the atop site, but theoretically prefers the hollow site [41]. In the case of the CN group in our experiments, the hollow site was the possible adsorption structure at Pt(1 1 1). Therefore, it is worthwhile to clarify what causes the difference of the preferential adsorption sites between the CN group and the CO molecule.

Except for Pt(1 1 1), the substrate dependence of the CPI adsorption geometry can be explained by the so-called d-band theory; the energy center of the valence d-band density of states at the surface sites correlates with their ability to form bonds with chemisorbed molecules [42,43]. The d-band center is calculated to be around −3.25 eV for Au and −1.5 eV for Pd [44], suggesting the preference of the atop and bridge adsorption at Au and Pd, respectively. On the other hand, the d-band center for Pt is known to be in the middle of Au and Pd [45], leading to coexistence of the atop and bridge configurations on Pt(1 0 0).

4. Conclusion

Significant enhancement of Raman scattering intensities of organic monolayers was demonstrated on non-SERS-active Pt and Pd surfaces. This enhancement method should be, in principle, effective not only for catalytic Pt-group metal but also for any other metals. The extension of the range of SERS application to observe non-SERS-active surfaces opens up a new possibility of SERS spectroscopy. In the case of this sphere-plane cavity system, its plasmonic resonance feature can be theoretically calculated and can be tuned by the sphere diameter. Therefore, one can easily obtain the maximum enhancement effect by matching the excitation energy and the plasmon resonance energy.

The application of the cavity to observe well-defined single crystal surfaces can also break the limitation of the conventional SERS spectroscopy. The preferential adsorption geometries of the isocyano group were clearly distinguished on each crystal face of the respective metals, which was impossible in conventional SERS. We have successfully decomposed the conventional SERS spectra at roughened Pt to the spectral components at (1 1 1) and (1 0 0) faces. This result is direct evidence that the low reproducibility in SERS is caused by the adsorption-site dependence of preferential molecular geometry on a metal surface. In principle, SERS spectroscopy has a great advantage for probing low-frequency vibrational modes such as molecule–substrate stretching especially in an IR-opaque solution. In situ SERS observations should be useful for study-

ing reaction mechanisms of electrocatalysts when adsorption-site selective Raman monitoring of molecular behavior is realized at a well-defined electrode surface. The gap-mode plasmon excitation method would improve our knowledge about catalytic reactions and electrochemical reactions.

Acknowledgments

This research was supported by Grant-in-Aid Scientific Research on Priority Area "Strong Photon-Molecule Coupling Fields" (Area No. 470, Grant No. 21020001), Grant-in-Aid for Young Scientists (B) (22750001), World Premier International Research Center (WPI) Initiative on Materials Nanoarchitechtonics, Global COE program (Project No. B01: Catalysis as the Basis for Innovation in Materials Science), and MEXT Program for Development of Environmental Technology using Nanotechnology from Ministry of Education, Culture, Sports, Science and Technology, Japan. We thank Dr. T. Okamoto (RIKEN) for technical assistance for calculating plasmonic properties.

References

[1] A. Otto, I. Mrozek, H. Grabhorn, W. Akemann, J. Phys.: Condens. Matter 4 (1992) 1143–1212.
[2] M. Moskovits, Rev. Modern Phys. 57 (1985) 783–826.
[3] M. Fleishmann, P.J. Hendra, A.J. McQuillan, Chem. Phys. Lett. 26 (1974) 163–166.
[4] D.L. Jeanmaire, R.P. Van Duyne, J. Electroanal. Chem. 84 (1977) 1–20.
[5] M.G. Albrecht, J.A. Creighton, J. Am. Chem. Soc. 99 (1977) 5215–5217.
[6] K. Kneipp, Y. Wang, H. Kneipp, L.T. Perelman, I. Itzkan, R.R. Dasari, M.S. Feld, Phys. Rev. Lett. 78 (1997) 1667–1669.
[7] S. Nie, S.R. Emory, Science 275 (1997) 1102–1106.
[8] H. Seki, J. Electron Spectrosc. Relat. Phenom. 39 (1986) 289–310.
[9] M. Futamata, E. Keim, A. Bruckbauer, D. Schumacher, A. Otto, Appl. Surf. Sci. 100/101 (1996) 60–63.
[10] M.E. Abdelsalam, P.N. Bartlett, J.J. Baumberg, A.E. Russell, J. Am. Chem. Soc. 129 (2007) 7399–7406.
[11] B. Pettinger, B. Ren, G. Picardi, R. Schuster, G. Ertl, Phys. Rev. Lett. 92 (2004) 096101.
[12] K. Ikeda, N. Fujimoto, H. Uehara, K. Uosaki, Chem. Phys. Lett. 460 (2008) 205–208.
[13] K. Ikeda, J. Sato, N. Fujimoto, N. Hayazawa, S. Kawata, K. Uosaki, J. Phys. Chem. C 113 (2009) 11816–11821.
[14] U. Jung, M. Müller, N. Fujimoto, K. Ikeda, K. Uosaki, U. Cornelissen, T. Felix, C. Bornholdt, D. Zargarani, R. Herges, O. Magnussen, J. Colloid Interface Sci. 341 (2010) 366–375.
[15] K. Ikeda, S. Suzuki, K. Uosaki, submitted for publication.
[16] K. Ikeda, K. Takahashi, T. Masuda, K. Uosaki, Angew. Chem. Int. Ed. 50 (2011) 1280–1284.
[17] P.K. Aravind, H. Metiu, J. Phys. Chem. 86 (1982) 5076–5084.
[18] P.K. Aravind, H. Metiu, Surf. Sci. 124 (1983) 506–528.
[19] R.T. Hill, J.J. Mock, Y. Urzhumov, D.S. Sebba, S.J. Oldenburg, S.-Y. Chen, A.A. Lazarides, A. Chilkoti, D.R. Smith, Nano Lett. 10 (2010) 4150–4154.
[20] J.F. Li, Y.F. Huang, Y. Ding, Z.L. Yang, S.B. Li, Z.S. Zhou, F.R. Fan, W. Zhang, Z.Y. Zhou, D.Y. Wu, B. Ren, Z.L. Wang, Z.Q. Tian, Nature 464 (2010) 392.
[21] J. Clavilier, R. Faure, G. Guinet, R. Durand, J. Electroanal. Chem. 107 (1980) 205–209.
[22] M.M. Wind, J. Vlieger, Physica A 141 (1987) 33–57.
[23] T. Okamoto, I. Yamaguchi, J. Phys. Chem. B 107 (2003) 10321–10324.
[24] P.B. Johnson, R.W. Christy, Phys. Rev. B 6 (1972) 4370–4379.
[25] D. Palik (Ed.), Handbook of Optical Constants of Solid, Academic Press, Orland, 1985.
[26] E. Prodan, C. Radloff, N.J. Halas, P. Nordlander, Science 302 (2003) 419–422.
[27] M.A. Ordal, R.J. Bell, R.W. Alexander Jr., L.L. Long, M.R. Querry, Appl. Opt. 24 (1985) 4493–4499.
[28] According to the DFT calculation, the molecular length of CPI on Au was estimated to be 0.9 nm.
[29] B. Pettinger, J. Chem. Phys. 85 (1986) 7442–7451.
[30] N.R. Avery, T.W. Matheson, Surf. Sci. 143 (1984) 110–124.
[31] S.M. Gruenbaum, M.H. Henney, S. Kumar, S. Zou, J. Phys. Chem. B 110 (2006) 4782–4792.
[32] K.L. Murphy, W.T. Tysoe, D.W. Bennett, Langmuir 20 (2004) 1732–1738.
[33] M. Ito, H. Noguchi, K. Ikeda, K. Uosaki, Phys. Chem. Chem. Phys. 12 (2010) 3156–3163.
[34] D.-H. Kang, M. Trenary, J. Am. Chem. Soc. 123 (2001) 8432–8433.
[35] K. Mudiyanselage, M. Trenary, R.J. Meyer, J. Phys. Chem. 112 (2008) 3794–3799.
[36] S. Katano, S. Kim, M. Hori, M. Trenary, M. Kawai, Science 316 (2007) 1883–1886.
[37] I. Nakamura, A. Takahashi, T. Fujita, Catal. Lett. 129 (2009) 400–403.
[38] J.P. Biberian, M.A. Van Hove, Surf. Sci. 118 (1982) 443–464.
[39] A. Brown, J.C. Vickerman, Surf. Sci. 124 (1983) 267–278.
[40] A.B. Anderson, Md.K. Awad, J. Am. Chem. Soc. 107 (1985) 7854–7857.
[41] G. Kresse, A. Gil, P. Sautet, Phys. Rev. B 68 (2003) 073401.
[42] B. Hammer, J.K. Nørskov, Surf. Sci. 343 (1995) 211–220.
[43] J. Greeley, J.K. Nørskov, M. Mavrikakis, Annu. Rev. Phys. Chem. 53 (2002) 319–348.
[44] A. Roudgar, A. Groß, J. Electroanal. Chem. 548 (2003) 121.
[45] V.R. Stamenkovic, B. Fowler, B.S. Mun, G. Wang, P.N. Ross, C.A. Lucas, N.M. Markovic, Science 315 (2007) 493–497.